

Automatic Segmentation of Different-Sized Leukoaraiosis Regions in Brain MR Images

Yoshikazu Uchiyama^a, Takuya Kunieda^a, Takeshi Hara^a, Hiroshi Fujita^a, Hiromichi Ando^b,
Hiroyasu Yamakawa^c, Takahiko Asano^d, Hiroki Kato^d, Toru Iwama^e, Masayuki Kanematsu^d,
Hiroaki Hoshi^d

^aDept. of Intelligent Image Information, Graduate School of Medicine, Gifu Univ., Japan

^bDept. of Neurosurgery, Gifu Municipal Hospital, Japan

^cDept. of Neurosurgery, Matsunami General Hospital, Japan

^dDept. of Radiology, Graduate School of Medicine, Gifu University, Japan

^eDept. of Neurosurgery, Graduate School of Medicine, Gifu University, Japan

ABSTRACT

Cerebrovascular diseases are the third leading cause of death in Japan. Therefore, a screening system for the early detection of asymptomatic brain diseases is widely used. In this screening system, leukoaraiosis is often detected in magnetic resonance (MR) images. The quantitative analysis of leukoaraiosis is important because its presence and extension is associated with an increased risk of severe stroke. However, thus far, the diagnosis of leukoaraiosis has generally been limited to subjective judgments by radiologists. Therefore, the purpose of this study was to develop a computerized method for the segmentation of leukoaraiosis, and provide an objective measurement of the lesion volume. Our database comprised of T1- and T2-weighted images obtained from 73 patients. The locations of leukoaraiosis regions were determined by an experienced neuroradiologist. We first segment cerebral parenchymal regions in T1-weighted images by using a region growing technique. For determining the initial candidate regions for leukoaraiosis, the k-means clustering of pixel values in the T1- and T2-weighted images was applied to the segmented cerebral region. For the elimination of false positives (FPs), we determined features such as the location, size, and circularity from each of the initial candidates. Finally, rule-based schemes and a quadratic discriminant analysis with these features were employed for distinguishing between the leukoaraiosis regions and the FPs. The results indicated that the sensitivity for the detection of leukoaraiosis was 100% with 5.84 FPs per image. Our computerized scheme can be useful in assisting radiologists for the quantitative analysis of leukoaraiosis in T1- and T2-weighted images.

Keywords: Magnetic resonance angiography (MRA), Leukoaraiosis, Clustering.

1. INTRODUCTION

Cerebrovascular diseases are the third leading cause of death in Japan.¹ Therefore, a screening system for the early detection of cerebral and cerebrovascular diseases, called *Brain Check-up*, is widely used in Japan. Because of the recent development in magnetic resonance imaging (MRI), various types of cerebral diseases such as lacunar infarct, unruptured aneurysm, occlusion, and leukoaraiosis have been detected by using this screening system. Therefore, we developed computer-aided diagnosis (CAD) schemes for the detection of the abovementioned diseases²⁻⁶ in order to assist radiologists who use the computer outputs as a guide in image interpretation.

Leukoaraiosis is frequently identified by the abovementioned screening system. The detection and management of leukoaraiosis is important because its presence and extension is associated with an increased risk of severe stroke. However, thus far, the diagnosis of leukoaraiosis has generally been limited to subjective judgments by radiologists. Therefore, the aim of our research was to develop a computerized method for the segmentation of leukoaraiosis, and provide an objective measurement of the lesion volume. Leukoaraiosis is one of the white matter diseases. There are many white matter diseases, for example, dementia and multiple sclerosis. Several

Corresponding author information: E-mail uchiyama@fjt.info.gifu-u.ac.jp.

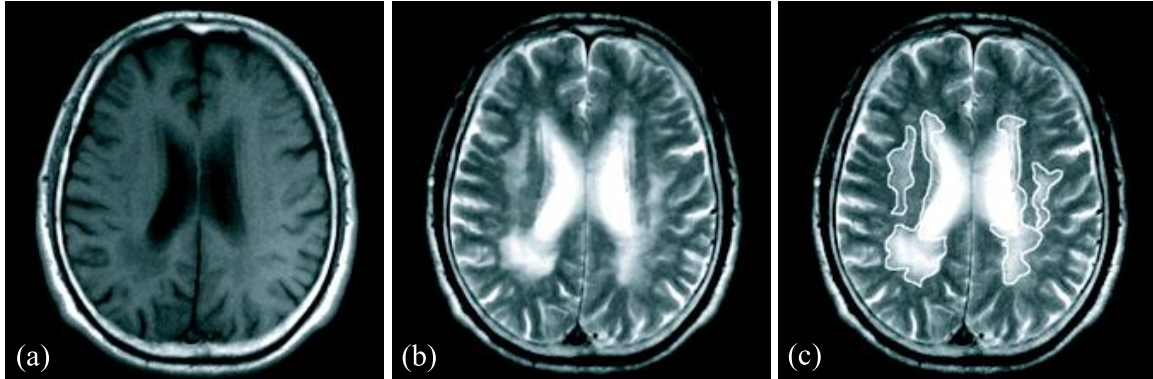


Figure 1. Examples of leukoaraiosis. (a) T1-weighted image. (b) T2-weighted image. (c) Leukoaraiosis regions determined by an experienced neuroradiologist superimposed on the T2-weighted image. The white lines indicate an abnormal area of leukoaraiosis. Leukoaraiosis exhibits high and relatively low signal intensities in T2- and T1-weighted images, respectively.

methods have been reported for the detection of dementia⁷ and multiple sclerosis.⁸ However, these diseases are not asymptomatic diseases. The difference between leukoaraiosis and multiple sclerosis is that the latter has various signal intensity values in a T1-weighted image and thus we required a different approach to segment these diseases. In the previous study on the detection of leukoaraiosis, a method based on the histogram of FLAIR images was proposed.⁹ However, an image phantom was used for evaluating the segmentation algorithm. Another study proposed a fuzzy interface system using a method that combined information from three different MR images: proton density, T2-weighted image, and FLAIR image.¹⁰ In this method, many steps were required to segment the leukoaraiosis regions.

In this study, we propose a method that uses the clustering technique for the detection of leukoaraiosis regions. Four image features for eliminating false positives (FPs) are also proposed. In addition, we will investigate the detection performance of our CAD schemes and demonstrate the usefulness of our methods for the detection of leukoaraiosis regions in T1- and T2-weighted images.

2. MATERIAL

Our database comprised of T1- and T2- weighted MR images obtained from 73 patients. These images were acquired using a 1.5T MR scanner (Symphony; SIEMENS) at Gero Hot Springs Hospital (Gero, Japan). The T1- and T2- weighted images were obtained using the first spin-echo method with an effective echo time of 14 milliseconds and 97 milliseconds, respectively, and a repetition time of 430 - 459 milliseconds and 3000 milliseconds, respectively. All MRIs were obtained in the axial plane with a section thickness of 5 mm and with a 2-mm intersection gap, which covered the entire brain. The matrix size of the MRIs was 512×512 , with a spatial resolution of 0.429 mm/pixel.

The leukoaraiosis regions in the images in our database were determined by an experienced neuroradiologist. We manually selected a slice with a lateral ventricle from each of the patient data, and used the slice images as an experimental dataset in this study. The dataset includes 53 normal slice images and 20 abnormal slices with 72 leukoaraiosis regions. Figure 1 shows an example of leukoaraiosis. Figures 1 (a) and (b) show T1- and T2-weighted images, respectively. The white lines in Figure 1(c) indicate an abnormal area of leukoaraiosis that was identified by an experienced neuroradiologist. Leukoaraiosis exhibits high and relatively low signal intensities in T2- and T1-weighted images, respectively. Figure 2 shows the distribution of the measured effective diameter for the 72 leukoaraiosis images. The effective diameter is defined as the diameter of the circle having the same area as the leukoaraiosis region. As shown in this figure, leukoaraiosis regions of various sizes are included in our dataset.

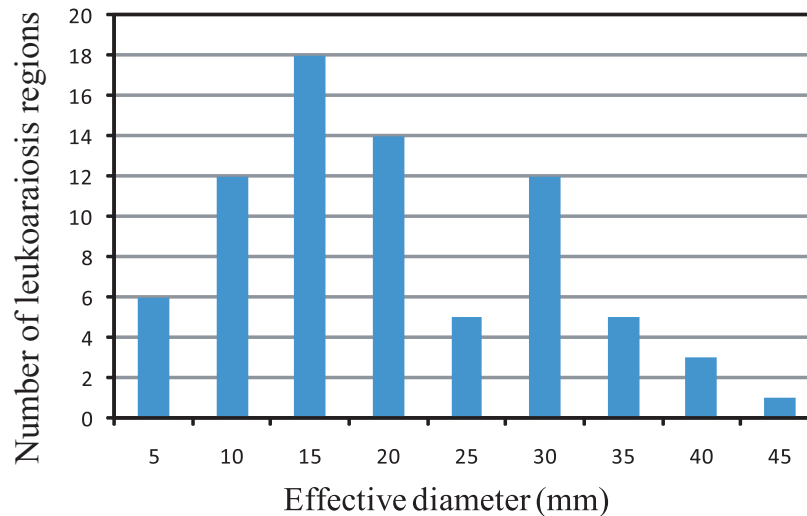


Figure 2. Distribution of effective diameters of 74 leukoaraiosis regions. The effective diameter is defined as the diameter of the circle having the same area as the leukoaraiosis region. Leukoaraiosis regions of various sizes are included in our dataset.

3. METHOD

3.1 Extraction of the Cerebral Parenchymal Region

In order to avoid detecting false findings located outside the cerebral region, we first segmented the cerebral parenchymal region using the region growing technique. We plotted a histogram of the T1-weighted image. All pixels of the brightest peak point in the histogram of the T1-weighted image were used as seed points. Figure 3 illustrates the process adopted for the extraction of the cerebral parenchymal region. Figures. 3 (a) and (b) show the original T1-weighted image and its histogram, respectively. The region was then grown by appending to each seed point when the difference between a point of interest and the value of the neighboring pixel was less than 15. Small islands were eliminated using size-based feature analysis. The remaining largest island was determined as the cerebral parenchymal region. Figure 3 (c) indicates the segmented cerebral parenchymal region by using the region growing method.

3.2 Determination of Initial Candidates for Leukoaraiosis

The signal intensity in MR image is a relative value and thus it changes for each patient. Therefore, it is difficult to directly use the signal intensity of an MR image as a thresholding value for detecting leukoaraiosis. However, leukoaraiosis has high and relative low signal intensity in T2- and T1-weighted images, respectively, and this characteristic remains the same for all patients. In this study, we employed a clustering method that used the pixel values of the T1- and T2-weighted images to determine the initial candidate regions for leukoaraiosis. Clustering is a method that classifies samples without the aid of a training set and can divide regions by merely using characteristics of pixel values in T1- and T2-weighted images. The k-means algorithm¹¹ was used to classify each pixel in the segmented cerebral parenchymal region into two regions. There were two clusters, i.e., leukoaraiosis and others. The pixel values of the T1- and T2-weighted images at the point of interest were used as input data. The k-means algorithm is based on two alternating procedures. First, pixels are assigned to groups. A pixel is usually assigned to a group to whose mean it is closest in the Euclidian sense in a 2D feature space having the pixel values of the T1- and T2-weighted image as two axes. Second, new group means are calculated based on the assignments. The process terminates when no pixel movement to another group will reduce the within-group sum of squares. The initial two cluster centers were given by the pixel values of the T1- and T2-weighted images in which the pixel has maximum and minimum values in the T2-weighted image. Figure 4 shows the effect of the clustering method for the detection of leukoaraiosis. Figure 4(a) and (b) show segmented cerebral parenchymal regions in T1- and T2-weighted images, respectively. As shown in these figures,

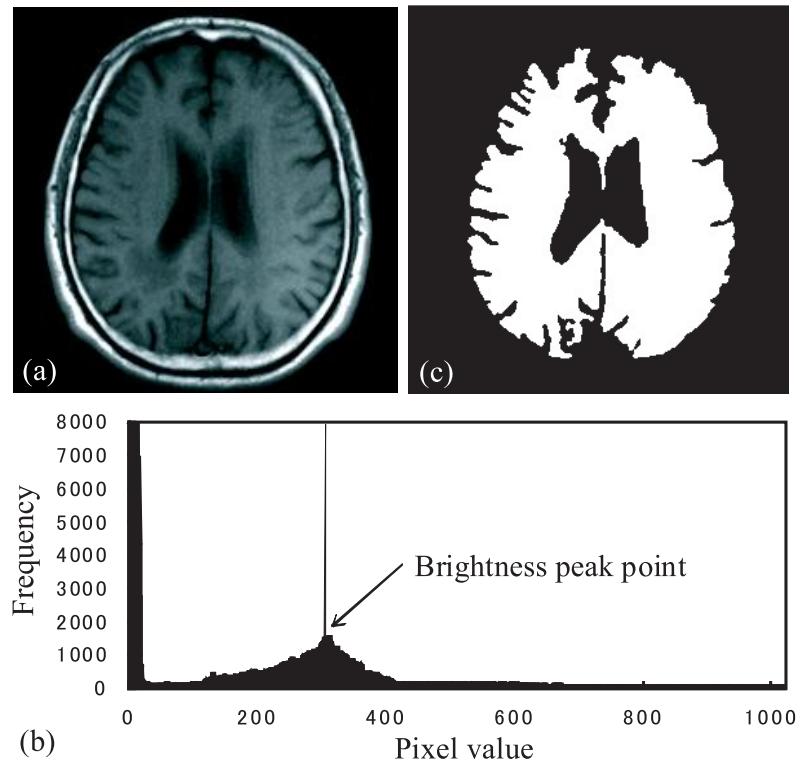


Figure 3. Extraction of the cerebral parenchymal region. (a) Original T1-weighted image. (b) Histogram of the T1-weighted image. (c) Extracted cerebral parenchymal region.

leukoaraiosis has high and relative low signal intensities in T2- and T1-weighted images, respectively. By using clustering methods, leukoaraiosis regions that have this characteristic were detected accurately. It should be noted that different-sized leukoaraiosis regions were also detected.

3.3 Features for Elimination of FPs

Using the technique described in the previous section, almost all leukoaraiosis regions were detected accurately. However, the candidates selected initially also include many FPs that were caused by a part of brain sulcus, a part of lateral ventricle, and so on. For eliminating these FPs, we used four features, i.e., location, size, circularity, and distance from the contour of the cerebral region.

Location

The x and y locations were defined based on the center of gravity in the candidate region. Leukoaraiosis occurs near the center of the cerebral region. Thus, the candidates located near the center of the cerebral region have a strong possibility of being leukoaraiosis regions. Based on the location, these candidates could be retained as true positives.

Size and circularity

The size was given as the number of pixels within the candidate region. The degree of circularity was defined by the fraction of the overlapping area of the candidate with the circle having the same area as the candidate. Because FPs due to a part of the cerebral ventricle are large in size and have irregular shapes, the size and circularity are useful features for eliminating these FPs.

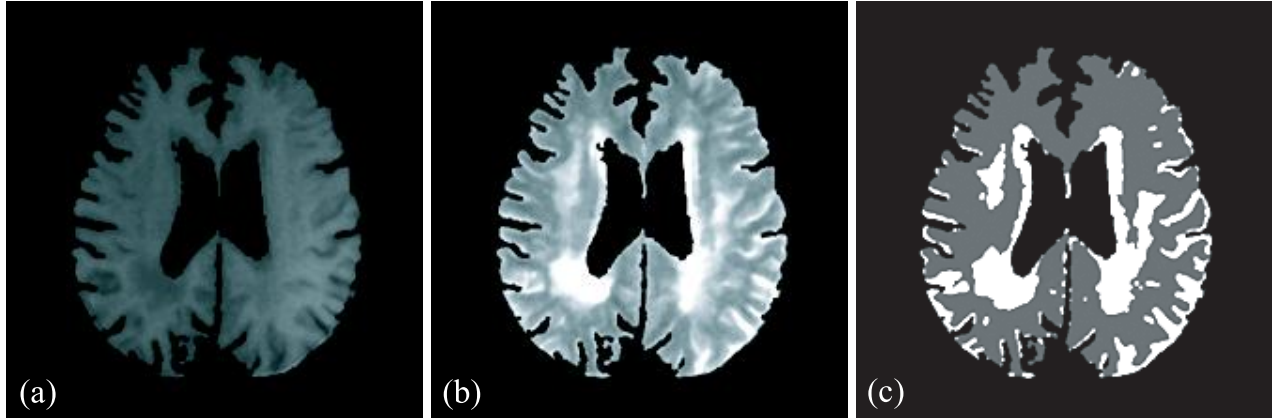


Figure 4. The effect of our leukoaraiosis detection method based on clustering technique. (a) Segmented cerebral region in the T1-weighted image. (b) Segmented cerebral regions in the T2-weighted image. (c) Result image of clustering technique. The white regions are the candidate regions obtained by the clustering technique. Almost all leukoaraiosis regions were detected accurately.

Distance from contour of cerebral region

In order to enhance the edge of the cerebral region, a Forsen filter¹² was first applied to the segmented cerebral parenchymal in section 3.1. A Forsen filter is defined by

$$g(x, y) = |f(x, y) - f(x + 1, y + 1)| + |f(x, y + 1) - f(x + 1, y)| \quad (1)$$

where $f(x, y)$ and $g(x, y)$ are the input and output images of the Forsen filter, respectively. Thresholding was then used for determining the outer edge of the cerebral region. The minimum Euclidian distance between the center of gravity in the candidate region and pixels on the outer edge of the cerebral region was calculated. The minimum distance was determined as the distance from the contour of the cerebral region. Since FPs are caused by a part of the brain sulcus located at the peripheral regions of the brain, the distance from the contour of the cerebral region is a useful feature for eliminating these FPs.

3.3.1 Elimination of FPs

A rule-based scheme with four features was employed as the first step in the elimination of FPs. In this scheme, we first calculated the maximum and minimum values of all leukoaraiosis regions detected in the initial step for identifying the leukoaraiosis candidates. All eight cutoff thresholds were then used for eliminating FPs (i.e., when a candidate was located outside the range determined by the cutoff threshold in the feature space, the candidate was considered to be an FP.)

For further eliminating FPs, we employed a three-layered artificial neural network (ANN) with a back-propagation algorithm.¹³ The numbers of input, hidden, and output units were 4, 4, and 1, respectively. The number of hidden units was determined empirically. The input data for the ANN was four features, which were the same as those in the rule-based schemes. The rule-based scheme was used to eliminate the outliers of FPs in the feature space. The ANN generates a decision boundary that optimally partitions the feature space into two classes, i.e., a leukoaraiosis class and FP class. The output value of the ANN indicates the likelihood of the occurrence of leukoaraiosis. For training and testing the ANN, the leave-one-out method was employed. By changing the threshold level of the output value, we can determine the detection performance using our computerized scheme.

4. RESULTS AND DISCUSSIONS

In order to investigate the performance of our CAD scheme, we applied it to 73 T1- and T2-weighted images with 74 leukoaraiosis regions in our dataset. As the first step toward identifying the initial candidates for leukoaraiosis,

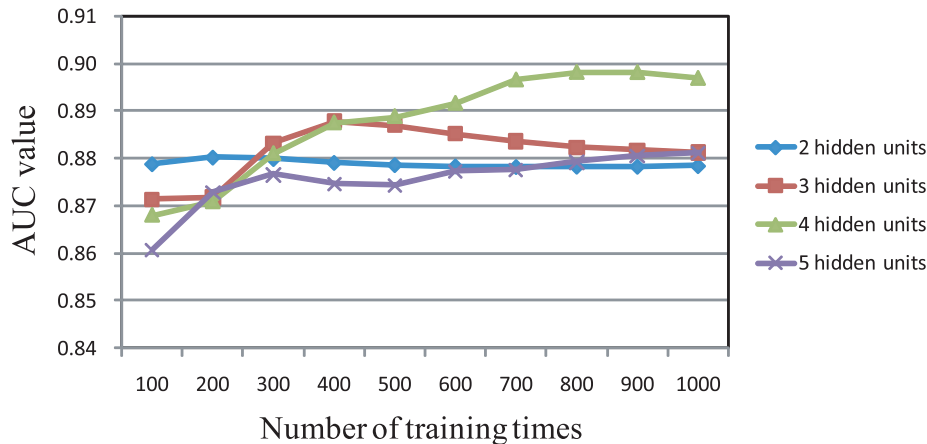


Figure 5. Relationship between the number of hidden units and the number of training time on the performance of our scheme by using a leave-one-out method. The performance of our scheme was evaluated by using the mean area under the best-fit binormal receiver operating characteristic (ROC) curves, which is called the AUC value.

100% of the (74/74) leukoaraiosis regions were accurately detected with 35.7 (2618/73) FPs per patient. This result indicates that k-means clustering was useful in the detection of leukoaraiosis regions because all such regions of various sizes were detected accurately. However, one problem is that many FPs were also detected using this method.

For the elimination of FPs, we determined four features from each of the initial candidates. These features were normalized using all cases in the dataset. By using the rule-based schemes with these four features, our CAD scheme achieved a sensitivity of 100.0% (74/74) with 9.0 (660/73) FPs per patient. Thus, 74.8% of the FPs were eliminated using this scheme. This result indicates that the features determined in this study were useful for distinguishing between the leukoaraiosis regions and the FPs.

For the further elimination of the FPs, an ANN with the same four features was employed for distinguishing between the leukoaraiosis regions and the FPs. To order to determine the appropriate number of training time and the number of hidden units, we investigated the effect of the change in the number of training times and the number of hidden units. Figure 5 shows the relationship between the number of hidden units and the number of training times on the performance of our scheme by using a leave-one-out method. The performance of our scheme was evaluated by using the mean area under the best-fit binormal receiver operating characteristic (ROC) curves,¹⁴ which is called the AUC value. In order to obtain the AUC values, we used the LABROC software developed by the University of Chicago.¹⁵ The optimal number of hidden units and the number of training time were determined as the values when the largest AUC value was obtained. By changing the output value of the ANN, we obtained the free-response receiver operating characteristic (FROC) curves.¹⁶ Figure 6 shows the FROC curves for the overall performance of the detection of leukoaraiosis. The results revealed that our CAD scheme achieved the same sensitivity of 100% (74/74) with 5.84 (427/73) FPs per patient. Although the sensitivity for the detection of leukoaraiosis regions was 100%, a problem that relative high FP rates was also obtained. Thus in the future, we need to improve our method for the elimination of these FPs.

5. CONCLUSIONS

We developed a computerized method for the segmentation of leukoaraiosis in T1- and T2-weighted MR images. The sensitivity of the detection of leukoaraiosis was 100% with 5.84 FPs per patients. Our computerized scheme can be useful in radiologists for the quantitative analysis of leukoaraiosis in T1- and T2-weighted images.

ACKNOWLEDGMENTS

This work was partly supported by a grant for the Knowledge Cluster Creation Project from the Ministry of Education, Culture, Sports, Science and Technology, Japan.

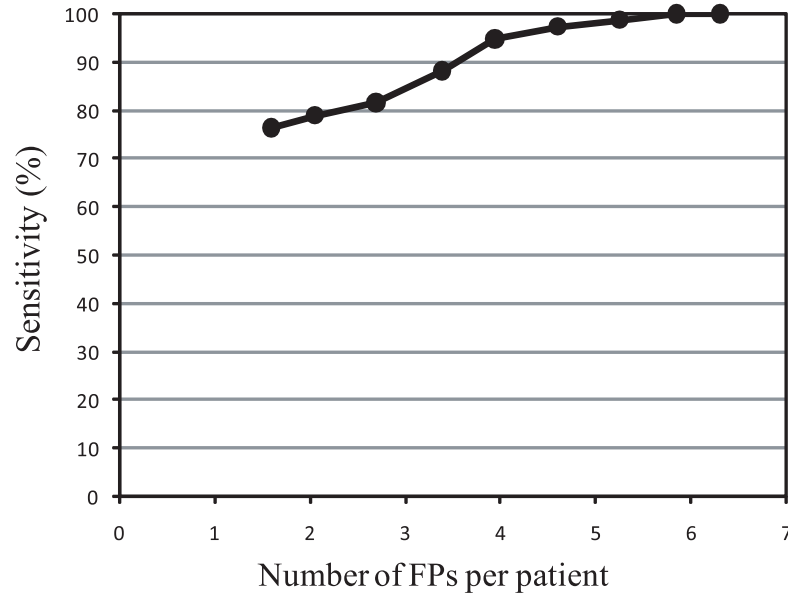


Figure 6. Free-response receiver operating characteristic (FROC) curve for the overall performance of our computer-aided detection scheme in the detection of leukoaraiosis. Our method evaluated based on a leave-one-out method. Our CAD scheme achieved a sensitivity of 100% with 5.84 FPs per patient.

REFERENCES

1. Health and W. S. Association, *Vital Statistics of Japan*, Daiwa Sougou Insatu, Tokyo, 2005.
2. R. Yokoyama, X. Zhang, Y. Uchiyama, H. Fujita, T. Hara, X. Zhou, M. Kanematsu, T. Asano, H. Kondo, S. Goshima, H. Hoshi, and T. Iwama, "Development of an automated method for detection of chronic lacunar infarct regions on brain MR images," *IEICE Trans. Inf. Syst.* **E90-D(6)**, pp. 943–954, 2007.
3. Y. Uchiyama, R. Yokoyama, H. Ando, T. Asano, H. Kato, H. Yamakawa, H. Yamakawa, T. Hara, T. Iwama, H. Hoshi, and H. Fujita, "Computer-aided diagnosis scheme for detection of lacunar infarcts on MR image," *Academic Radiology* **14(12)**, pp. 1554–1561, 2007.
4. Y. Uchiyama, H. Ando, R. Yokoyama, T. Hara, H. Fujita, and T. Iwama, "Computer-aided diagnosis scheme for detection of unruptured intracranial aneurysms in MR angiography," *Proc of IEEE Engineering in Medicine and Biology 27th Annual International Conference* **1**, pp. 3031–3034, 2005.
5. Y. Uchiyama, M. Yamauchi, H. Ando, R. Yokoyama, T. Hara, H. Fujita, T. Iwama, and H. Hoshi, "Automated classification of cerebral arteries in MRA images and its application to maximum intensity projection," *Proc of IEEE Engineering in Medicine and Biology 28th Annual International Conference* **1**, pp. 4865–4868, 2006.
6. M. Yamauchi, Y. Uchiyama, R. Yokoyama, T. Hara, H. Fujita, H. Ando, H. Yamakawa, T. Iwama, and H. Hoshi, "Computerized scheme for detection of arterial occlusion in brain MRA images," *Proc. of SPIE Medical Imaging : Computer-Aided Diagnosis* **6514**, pp. 65142C–1–65142C–9, 2007.
7. A. P. Zijdenbos, B. M. Dawant, R. A. Margolin, and C. A. Palmer, "Morphometric analysis of white matter lesions in mr images: method and validation," *IEEE Transaction on Medical Imaging* **13(4)**, pp. 716–724, 1994.
8. A. Charil, A. P. Zijdenbos, J. Taylor, C. Boelman, K. J. Worsley, A. C. Evans, and A. Dagher, "Statistical mapping analysis of lesion location and neurological disability in multiple sclerosis: application to 452 patient data sets," *NeuroImage* **19**, pp. 532–544, 2003.
9. R. J. Clifford, P. C. O'Brien, D. W. Rettman, M. M. Shiung, Y. Xu, R. Muthupillai, A. Manduca, R. Avula, and B. J. Erickson, "FLAIR histogram segmentation for measurement of leukoaraiosis volume," *Journal of Magnetic Resonance Imaging* **14**, pp. 668–676, 2001.

10. F. Adamiraa-Behloul, D. M. J. van den Heuvel, H. O. M. J. P. van Osch, J. van der Grond, M. A. van Buchem, and J. H. C. Reiber, "Fully automatic segmentation of white matter hyperintensities in MR images of the elderly," *NeuroImage* **28**, pp. 607–617, 2005.
11. R. O. Duda, E. H. Hart, and D. G. Stork, *Pattern Classification*, John Wiley & Sons, Inc., New York, 2001.
12. W. K. Pratt, *Digital Image Processing*, John Wiley & Sons, Inc., New York, 1991.
13. S. Haykin, *Neural network: comprehensive foundation*, Prentice-Hall, Englewood Cliffs, NJ, 1999.
14. C. E. Metz, B. A. Herman, and J. H. Shen, "Maximum likelihood estimation of receiver characteristics (ROC) curves from continuously-distributed data," *Statistics in Medicine* **17**, pp. 1033–1053, 1998.
15. <http://www-radiology.uchicago.edu/krl/>.
16. D. P. Chakraborty, "Maximum likelihood analysis of free-response receiver operating characteristic (FROC) data," *Medical Physics* **16(4)**, pp. 561–568, 1989.